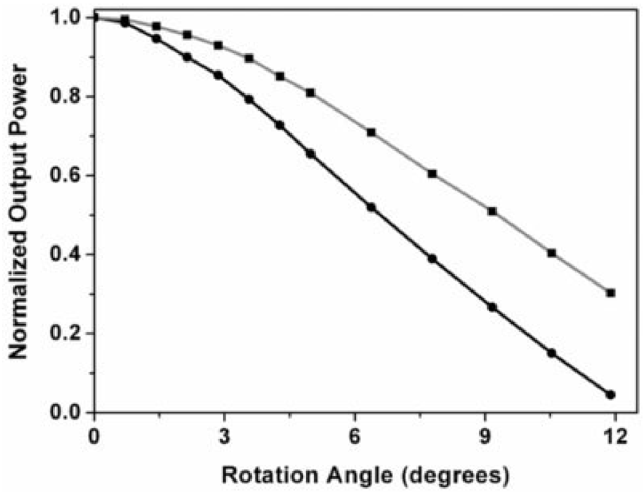

Figure 4 Measured normalized output power as a function of the tilt angle

3. RESULTS AND DISCUSSION

Figure 4 shows the normalized output power against the tilt angle with FBG (squares). The normalized output power shows a monotonic decrement against the tilt angle, as expected. For comparison, the normalized output power against the tilt angle without FBG was also measured, and the results are given in Figure 4 (circles). From the results, we can see that the FBG can effectively enhance the tilt angle sensitivity of the sensor.

The Bragg wavelength shift of the FBG with temperature was directly recorded by monitoring the wavelength shift using an optical spectrum analyzer. The resolution of the optical spectrum analyzer is limited (0.01 nm). The temperature response of the senor is shown in Figure 5. A sensitivity of about 0.0121 nm/°C was obtained. The temperature sensitivity of the sensor can be enhanced by packaging with a material with higher temperature sensitivity.

4. CONCLUSION

A sensor based on a fiber taper and an FBG for simultaneous measurement of the tilt angle and temperature has been presented. The sensor is operated in the reflection mode. The magnitude of the tilt angle can be obtained by monitoring the tilt-induced loss of the light that passes the taper and is reflected by the FBG. The fiber grating can not only enhance the tilt angle sensitivity but also measure the surrounding temperature by the wavelength shift. The sensor is simple and compact.

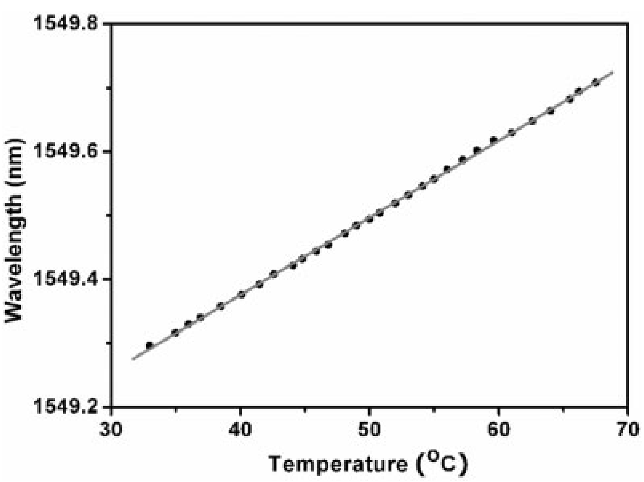

Figure 5 Measured wavelength shift as the surrounding temperature varies

ACKNOWLEDGMENT

This work was partially supported by Zhejiang provincial government (under grant No. 2004C31G2010019) and Hangzhou municipal government (under grant No. 20051321B14).

REFERENCES

1. B.S. Kawasaki, K.O. Hill, and R.G. Lamont, Biconical-taper single mode fiber coupler, Opt Lett 6 (1981), 327–328.
2. K.P. Jedrzejewski, F. Martinez, J.D. Minelly, C.D. Hussey, and F.P. Payne, Tapered-beam expander for single-mode optical-fibre gap devices, Electron Lett 22 (1986), 105–106.
3. A.B. Timothy and W. L. Youwei, The shape of fiber tapers, IEEE J Light Technol 10 (1992), 432–438.
4. S. Rabbany et al., Optical immunosensor, Crit Rev Biomed Eng 22 (1994), 307–346.
5. T. Allsop, F. Floreani, K. Jedrzejewski, P. Marques, R. Romero, D. Webb, and I. Bennion, Refractive index sensing with long-period grating fabricated in biconical tapered fibre, Electron Lett 41 (2005), 471–472.
6. F.L. Arregui et al., Optical fiber strain gauge based on a tapered single mode fiber, Sens Actuators A 79 (2000), 90–96.
7. A.D. Kersey, M.A. Davis, J. Patrick, M. LeBlanc, K.P. Koo, C.G. Askins, M.A. Putnam, and E.J. Friebele, Fiber grating sensors, IEEE J Light Technol 15 (1997), 1442–1463.
8. T.A. Berkoff and A.D. Kersey, Experimental demonstration of a fiber Bragg grating accelerometer, IEEE Photon Technol Lett 8 (1996), 1677–1679.
9. N. Takahashi, K. Yoshimura, S. Takahashi, and K. Imamura, Characteristics of fiber Bragg grating hydrophone, IEICE Trans Electron E83–C (2000), 275–281.
10. L.C. Bobb, P.M. Shankar, and H.D. Krumboltz, Bending effects in biconically tapered single-mode fibers, IEEE J Light Technol Lett 8 (1990), 1084–1090.
11. A.J. Harris and P.F. Castle, Bend loss measurements on high numerical aperture single-mode fibers as a function of wavelength and bend radius, IEEE J Light Technol 4 (1986), 34–40.
12. R.J. Black and R. Bourbonnais, Core-mode "cutoff" for finite-cladding lightguides, IEE Proc J Optoelectron 133 (1986), 377–384.

SURFACE-MOUNT LOOP ANTENNA FOR AMPS/GSM/DCS/PCS OPERATION IN THE PDA PHONE

Wei-Yu Li and Kin-Lu Wong
Department of Electrical Engineering, National Sun Yat-Sen University, Kaohsiung 804, Taiwan, Republic of China

Received 27 February 2007

ABSTRACT: *A surface-mount loop antenna very suitable for application in the mobile devices such as the PDA (Personal Digital Assistant) phone for quad-band operation is presented. The antenna comprises of a loop metal pattern for generating two wideband resonant modes at about 900 and 1800 MHz to cover the AMPS/GSM/DCS/PCS bands and a central coupling stub as the feed structure. Although quad-band operation is obtained, the antenna occupies a small volume of $7 \times 8 \times 60$ mm^3 or about 3.4 cm^3 only and is easy to be embedded inside the PDA phone as an internal antenna. Details of the proposed surface-mount* *loop antenna are presented and discussed.* © 2007 Wiley Periodicals, Inc. Microwave Opt Technol Lett 49: 2250–2254, 2007; Published online in Wiley InterScience (www.interscience.wiley.com). DOI 10.1002/mop.22700

Key words: *PDA phone antennas; mobile phone antennas; surface-mount antennas; loop antennas; multiband antennas*

1. INTRODUCTION

It has been known that when the loop antenna is operated at its balanced one-wavelength mode, small excited surface currents on the ground plane attached to the antenna can be obtained [1, 2]. With this attractive property, when such a loop antenna is applied to the mobile device, effects of the nearby environments such as the user's hand holding the device on the antenna performances are expected to be greatly reduced. This property is advantageous over the conventional internal mobile device antennas in the forms of the planar inverted-F patch antenna, very-low-profile printed or metal-plate monopole antenna, and the like [3]. For this reason, promising designs of the loop antenna for application in the mobile device have been reported [4-12]. Many designs for achieving single-band operation have been demonstrated [4-8]. There are also some interesting designs for achieving dual-band or multiband operation [9-12]. Owing to the rapid growth in mobile communications, the compact loop antennas capable of multiband operation are expected to be very attractive for practical applications in the mobile devices.

In this article, we present a new surface-mount loop antenna capable of quad-band operation covering the AMPS (Advanced Mobile Phone System, 824–894 MHz), GSM (Global System for Mobile Communication, 890–960 MHz), DCS (Digital Communication System, 1710–1880 MHz), and PCS (Personal Communication System, 1850–1990 MHz) bands. The surface-mount loop antenna comprises of a meandered loop metal pattern and a central coupling stub to capacitively excite the meandered loop for quad-band operation. The antenna configuration is simple, which allows it easy to fabricate. In this study, the antenna is mounted on the surfaces of a small foam base, and it is very appropriate to be embedded inside the casing of the mobile device to operate as an internal antenna. In addition, with the surface-mount technology, the packaging cost of the final product can be reduced [13]. Details of the proposed quad-band surface-mount loop antenna are presented, and the example of the antenna applied to a smart phone or Personal Digital Assistant (PDA) phone is studied.

2. ANTENNA DESIGN

Figure 1(a) shows the geometry of the surface-mount loop antenna for quad-band operation, and the metal pattern of the antenna in the planar structure is shown in Figure 1(b). The antenna is to be surface-mounted at the top, no-ground portion (area 7 × 60 mm^2) of the system circuit board (area 97 × 60 mm^2) of the PDA phone. In this study, a 0.8-mm thick FR4 substrate is used as the circuit board. On the back side of the circuit board there is a ground plane (area 90 × 60 mm^2) printed. These selected dimensions are reasonable for general smart phones or PDA phones.

The antenna mainly comprises a loop metal pattern and a central coupling stub. In the study, the loop metal pattern and coupling stub are obtained by line-cutting from a copper plate; then, they are attached onto the surfaces of a foam base (size 7 × 8 × 60 mm^3) as shown in the figure or similar to those studied in [14, 15]. The loop metal pattern is meandered at its two side sections to achieve a longer length (about 185 mm from point B to point C) on the fixed surfaces of the foam base. The length of the loop metal pattern is close to about one wavelength of the frequency at 1800 MHz; this can lead to the excitation of a full-wavelength resonant mode at about 1800 MHz to cover the DCS and PCS bands. In addition, a half-wavelength resonant mode is also found to be excited at about 900 MHz to cover the AMPS and GSM bands.

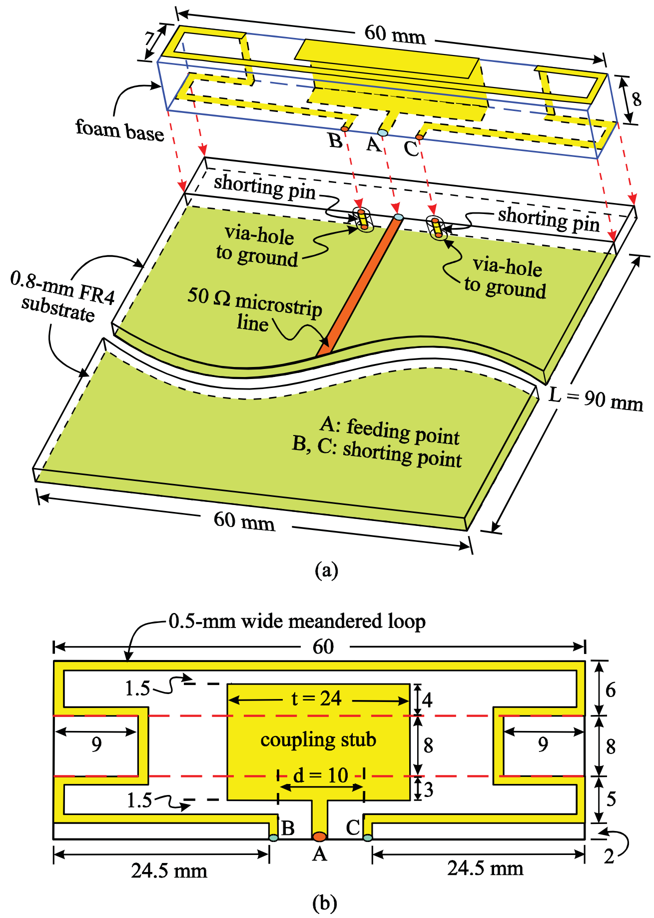

Figure 1 (a) Geometry of the proposed quad-band surface-mount loop antenna for the PDA phone. (b) The metal pattern of the antenna in the planar structure. [Color figure can be viewed in the online issue, which is available at www.interscience.wiley.com]

The central coupling stub has a rectangular shape of length 15 mm and width 24 mm (t). There are small coupling gaps of width 1.5 mm between the coupling stub and the loop metal pattern, and a 50-Ω microstrip line printed on the circuit board is connected to the coupling stub at the feeding point (point A). The small coupling gaps lead to good coupling of the input power from the microstrip feedline to the antenna. By selecting proper values of the distance d (10 mm) between two short-circuited ends (point B and point C) of the loop metal pattern and the width t (24 mm) of the coupling stub, improved impedance matching of the two wideband resonant modes at about 900 and 1800 MHz can be obtained.

3. RESULTS AND DISCUSSION

The proposed antenna with dimensions given in Figure 1 was fabricated and tested. Figure 2 shows the measured and simulated return loss of the constructed prototype. The simulated results are obtained using Ansoft HFSS [16], and agreement between the measurement and simulation is obtained. There are two wideband resonant modes excited, which are the half- and one-wavelength modes of the studied loop antenna. The lower mode at about 900 MHz shows a large bandwidth of 490 MHz (810–1300 MHz),

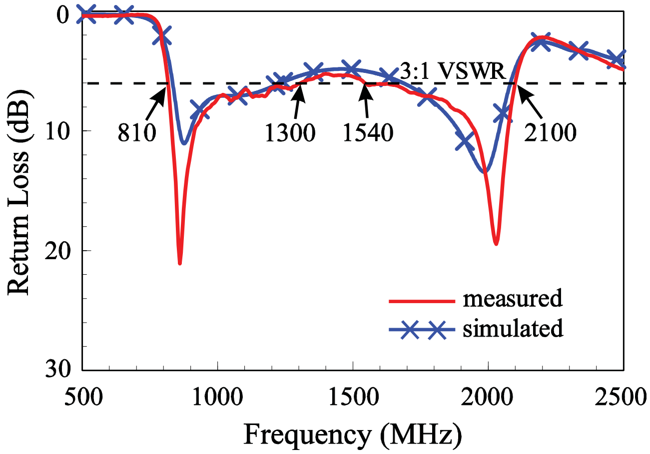

Figure 2 Measured and simulated return loss for the proposed antenna. [Color figure can be viewed in the online issue, which is available at www.interscience.wiley.com]

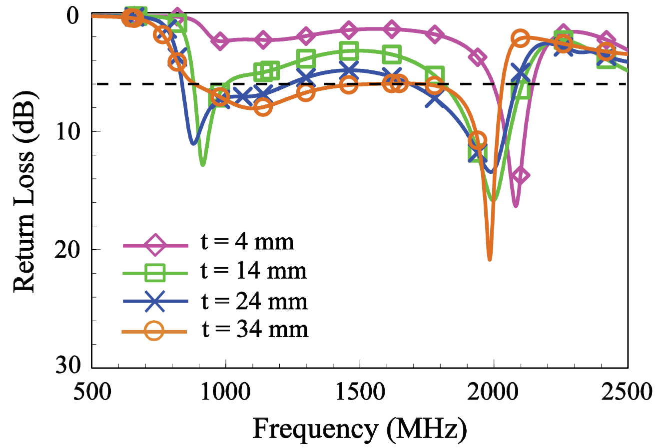

Figure 4 Simulated return loss as a function of *t*; other parameters are the same as given in Figure 1. [Color figure can be viewed in the online issue, which is available at www.interscience.wiley.com]

allowing the antenna to easily cover the AMPS and GSM bands. The bandwidth is defined by 3:1 VSWR or 6-dB return loss, which is generally used for the mobile phone antennas in practical applications. For the upper mode, it shows a large bandwidth of 560 MHz (1540–2100 MHz) covering the DCS and PCS bands.

Effects of the distance *d* are studied in Figure 3, and the results for *d* varied from 6 to 18 mm are presented. Much larger effects on the upper mode are seen. The center frequency of the upper mode is shifted to higher frequencies when the distance *d* is increased. This is largely because the increase in *d* will lead to the decrease in the total length of the loop metal pattern. The center frequency of the upper mode which is a balanced one-wavelength resonant mode will thus be increased. For the lower mode, which is an unbalanced half-wavelength resonant mode, smaller effects are reasonable. This is because in this case the ground plane also plays an essential part in the excitation of the lower mode; thus the variations in the distance *d* alone will have smaller effects on the lower mode.

Figure 4 shows the effects of the width *t* on the antenna performance. Large effects on both the lower and upper bands are observed. There exists a proper value of *t* (24 mm here) for the two modes, especially for the lower mode. Effects of the groundplane length *L* on the antenna performance are also studied, and the results for *L* varied from 80 to 95 mm are shown in Figure 5. In this case much larger effects on the lower mode are seen. This behavior is reasonable, because the lower mode is operated as an unbalanced resonant mode, and thus it will be more sensitive to the variations in the groundplane length [17, 18] than the upper mode. However, for $L = 85$ mm, the obtained bandwidth of the lower mode can still cover the AMPS and GSM bands.

Radiation characteristics of the proposed antenna are also studied. Figure 6 plots the measured radiation patterns at 890 MHz, about the center frequency of the AMPS/GSM bands (824–960 MHz). At 890 MHz, monopole-like radiation patterns are seen, and the radiation patterns for frequencies over the AMPS/GSM bands are also about the same as those plotted here. The radiation pattern is similar to those observed for the conventional internal mobile phone antenna with an unbalanced structure for GSM operation [3].

The measured radiation patterns at 1850 MHz, center frequency of the DCS/PCS bands (1710–1990 MHz) bands, are shown in Figure 7. The radiation patterns for other frequencies over the DCS/PCS bands also show small variations as plotted here. More variations in the radiation patterns are seen, which is owing to

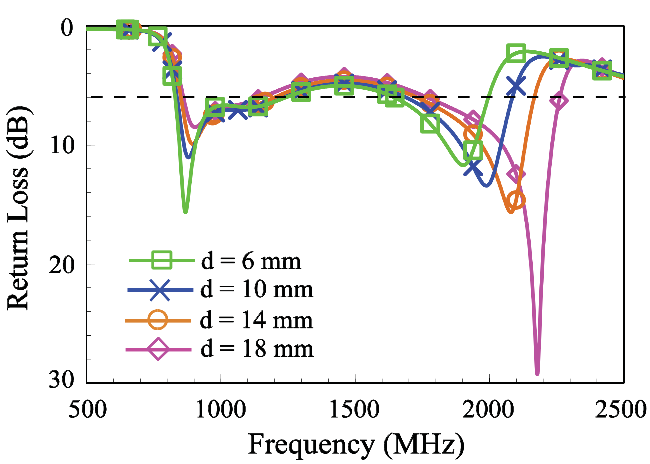

Figure 3 Simulated return loss as a function of *d*; other parameters are the same as given in Figure 1. [Color figure can be viewed in the online issue, which is available at www.interscience.wiley.com]

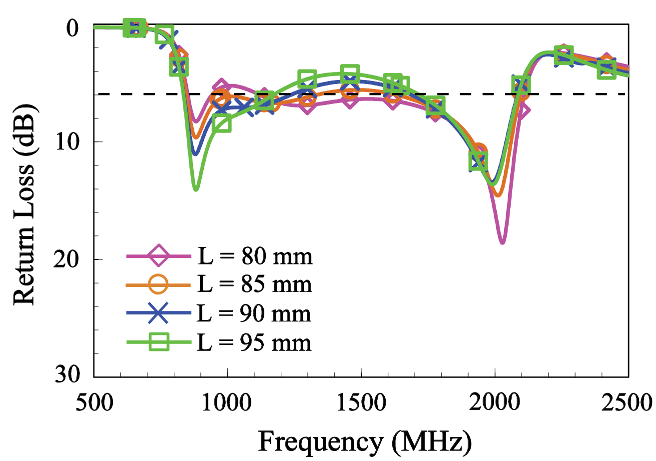

Figure 5 Simulated return loss as a function of the groundplane length *L*; other parameters are the same as given in Figure 1. [Color figure can be viewed in the online issue, which is available at www.interscience.wiley.com]

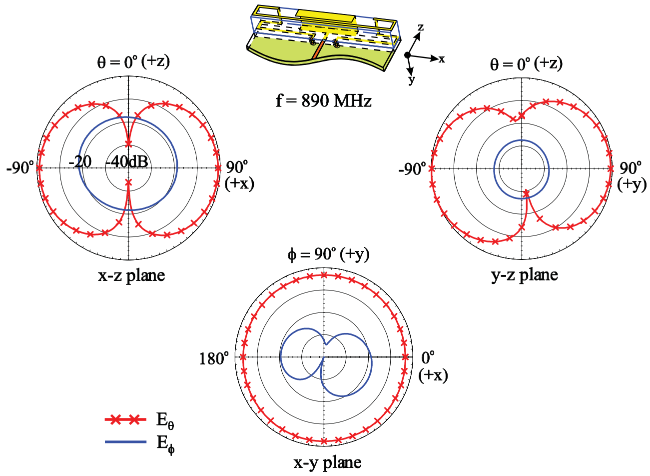

Figure 6 Measured radiation patterns at 890 MHz for the proposed antenna. [Color figure can be viewed in the online issue, which is available at www.interscience.wiley.com]

more nulls in the excited surface currents along the loop metal pattern excited as a one-wavelength resonant mode. In the *x–y* plane, the azimuthal plane, symmetric radiation pattern is seen, which is largely owing to the symmetric structure of the loop metal pattern and the excitation of the antenna at its central part.

The measured maximum antenna gain and simulated radiation efficiency are presented in Figure 8. For the lower mode shown in Figure 8(a), the antenna gain varies from about −0.4 to 1.2 dBi for the AMPS band and is stable with a value of about 1.0 dBi for the GSM band. For the efficiency, it is about 58–75% for the AMPS band and about 75% over the GSM band. For the upper band shown in Figure 8(b), the antenna gain varies from about 1.8–3.6 dBi for the DCS band and about 3.2–3.8 dBi for the PCS band. The efficiency is about 70–80% over the DCS band and 78–82% over the PCS band.

4. CONCLUSION

A quad-band surface-mount loop antenna for AMPS/GSM/DCS/PCS operation in the smart phone or PDA phone has been demonstrated. The loop antenna is supported by a foam base and is

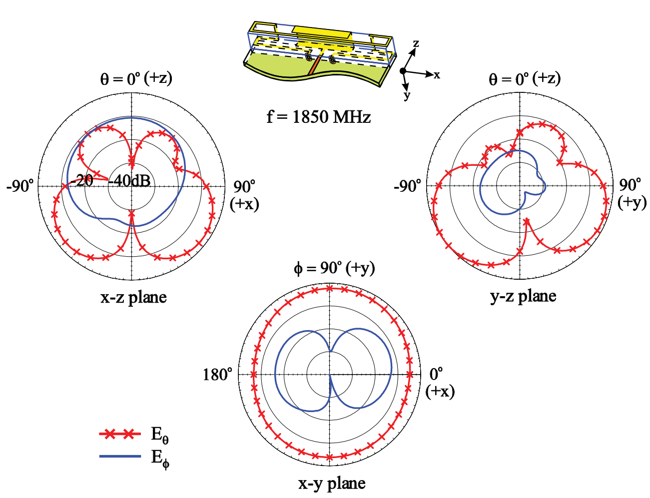

Figure 7 Measured radiation patterns at 1850 MHz for the proposed antenna. [Color figure can be viewed in the online issue, which is available at www.interscience.wiley.com]

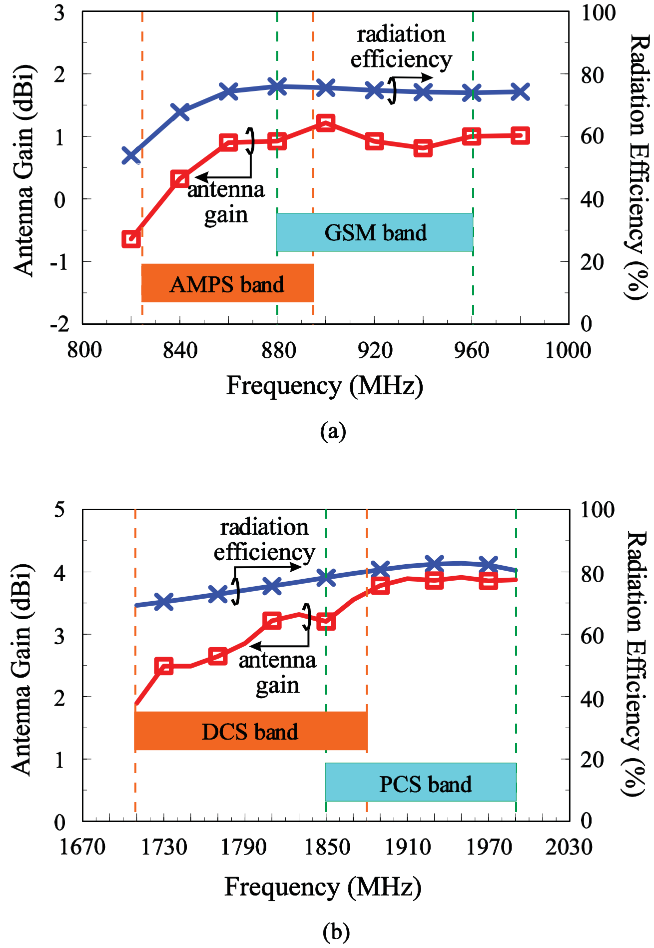

Figure 8 Measured maximum antenna gain and simulated radiation efficiency over (a) the AMPS/GSM bands and (b) the DCS/PCS bands. [Color figure can be viewed in the online issue, which is available at www.interscience.wiley.com]

suitable to be surface-mounted on the no-ground portion of the system circuit board of the PDA phone. The loop antenna is excited using a central coupling stub, and two wideband resonant modes are excited at about 900 and 1800 MHz to cover the AMPS/GSM and DCS/PCS bands. The lower mode is an unbalanced half-wavelength mode, while the upper mode is a balanced one-wavelength mode. Their impedance and radiation characteristics have been studied, and good antenna performances for the quad-band operation have been obtained. It is also promising to replace the foam base with a ceramic base for the proposed antenna; in this case, the antenna volume can be reduced, and however, the obtained bandwidth may be decreased. The possible structure with a ceramic base will be investigated in the future study.

REFERENCES

1. H. Morishita, Y. Kim, and K. Fujimoto, Design concept of antennas for small mobile terminals and the future perspective, IEEE Antennas Propag Mag 44 (2002), 30-43.
2. H. Morishita, H. Furuuchi, and K. Fujimoto, Performance of balanced-Fed antenna system for handsets in the vicinity of a human head or hand, IEE Proc Microwave Antennas Propag 149 (2002), 85-91.
3. K.L. Wong, Planar antennas for wireless communications, Wiley, New York, USA, 2003.
4. K.D. Katsibas, C.A. Balanis, P.A. Tirkas, and C.R. Birtcher, Folded

loop antenna for mobile hand-held units, IEEE Trans Antennas Propag 46 (1998), 260-266.
5. T. Adachi, A Hirata, and T. Shiozawa, Folded-loop antennas for handset terminals at the 2.0-GHz band, Microwave Opt Technol Lett 36 (2003), 376-378.
6. K.L. Wong, A.C. Chen, and F.S. Chang, Planar diversity loop antenna for wireless PCMCIA card, Microwave Opt Technol Lett 39 (2003), 488-490.
7. S. Hayashida, T. Tanaka, H. Morishita, Y. Koyanagi, and K. Fujimoto, Built-in folded monopole antenna for handsets, Electron Lett 40 (2004), 1514-1516.
8. C.C. Chiau, X. Chen, and C.G. Parini, A miniature dielectric-loaded folded half-loop antenna and ground plane effects, IEEE Antennas Wireless Propag Lett 4 (2005), 459-462.
9. C.C. Lin, G.Y. Lee, and K.L. Wong, Surface-mount dual-loop antenna for 2.4/5 GHz WLAN operation, Electron Lett 39 (2003), 1301-1302.
10. C.H. Kuo, K.L. Wong, and F.S. Chang, Internal GSM/DCS dual-band open-loop antenna for laptop application, Microwave Opt Technol Lett 49 (2007), 680-684.
11. B. Jung, H. Rhyu, Y.J. Lee, F.J. Harackiewwicz, M.J. Park, and B. Lee, Internal folded loop antenna with tuning notches for GSM/GPS/DCS/PCS mobile handset applications, Microwave Opt Technol Lett 48 (2006), 1501-1504.
12. C.I. Lin and K.L. Wong, Internal meandered loop antenna for GSM/DCS/PCS multiband operation in a mobile phone with the user's hand, Microwave Opt Technol Lett 49 (2007), 759-765.
13. Y. Dakeya, T. Suesada, K. Asakura, N. Nakajima, and H. Mandai, Chip multilayer antenna for 2.45 GHz-band application using LTCC technology, IEEE MTT-S Int Microwave Symp, Boston, MA (2000), 1693-1696.
14. K.L. Wong and C.H. Chang, Surface-mountable EMC monopole chip antenna for WLAN operation, IEEE Trans Antennas Propag 54 (2006), 1100-1104.
15. K.L. Wong and C.H. Chang, WLAN chip antenna mountable above the system ground plane of a mobile device, IEEE Trans Antennas Propag 53 (2005), 3496-3499.
16. Ansoft Corporation HFSS, http://www.ansoft.com/products/hf/hfss/.
17. T.Y. Wu and K.L. Wong, On the impedance bandwidth of a planar inverted-F antenna for mobile handsets, Microwave Opt Technol Lett 32 (2002), 249-251.
18. P. Vainikainen, J. Ollikainen, O. Kivekas, and I. Kelander, Resonator-based analysis of the combination of mobile handset antenna and chassis, IEEE Trans Antennas Propagat 50 (2002), 1433-1444.

FINLINE TAPERS USING CLOSED-FORM EXPRESSIONS FOR MILLIMETER WAVE INTEGRATED SYSTEMS

Ashok Mittal[1] **and Asok De**
Delhi College of Engineering, Delhi 110 042, India

Received 1 February 2007

ABSTRACT: *Conventional techniques for designing waveguide-to-finline taper transitions are based on the design of a suitable impedance transformation profile used for pure TEM lines. Change of finline/slotline gap not only causes change in impedance but also correspondingly change in propagation constant. Thus the existing analysis, used for purely TEM lines, is inadequate in dealing with finline tapers. Analysis has also been carried out by varying the propagation constant using closed-form expressions. Comparison of various taper profiles has been presented in this paper. Further in the present work, the width of the finline contour itself has been varied according to the function profiles as exponential, parabolic, cosine, and cosine squared forming the tapers. Broadband tapered transition from rectangular waveguide to offset slot asymmetric finline has been realized by gradually increasing the slot width using exponential taper profile. The designed asymmetric finline taper (two transition with one lambda spacing) using impedance variation with width exponential profile showed a very good result of 0.15–0.25 dB in the entire Ka-band.* © 2007 Wiley Periodicals, Inc. Microwave Opt Technol Lett 49: 2254–2257, 2007; Published online in Wiley InterScience (www.interscience.wiley.com). DOI 10.1002/mop.22688

Key words: *millimeter wave; finline; tapers; transitions; waveguide transitions; finline transitions*

1. INTRODUCTION

In microwave and millimeter wave circuits, the interconnection between chips and packaging of the whole system is always fundamentally important. When the operating frequency approaches at millimeter wave frequencies, waveguide interconnection between chips, i.e. chip in waveguide, is more preferable because of its inherent low transmission losses. In order to couple energy from waveguide to a millimeter wave monolithic integrated circuit (MMIC) on a chip, some kind of impedance transformation is required. Although a quarter-wave transformer could theoretically be used, a good performance is difficult to achieve. The operational bandwidth of a quarter-wave transformer could be very narrow and is difficult to predict accurately with the available accuracy of the measurements of the impedance and propagation constant of the slotline that is placed inside a waveguide. Therefore, a preferable solution is to employ a tapered finline, which gives broader bandwidth. Many authors have presented their analysis for various taper contours connecting rectangular waveguide to finlines [1–5]. Broadband transitions from rectangular waveguide to finlines are made by using tapered finline, i.e. slot width is gradually increased from slotline to full waveguide height (Fig. 1).

Most of the designs reported for the finline tapers involve choice of smooth impedance variation along the tapered line so that the reflection loss is below a tolerable limit over a wide bandwidth. Most of the analysis presented is centered on the TEM structures by taking propagation constant β as constant, whereas finline is a non-TEM line and propagation constant β is also a function of z. In the present analysis, propagation constant β is also varied using closed-form expressions and the reflection coefficient response of various taper profiles has been presented.

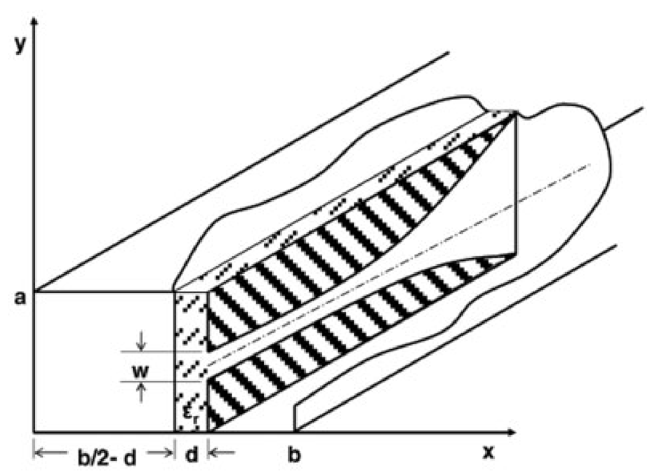

Figure 1 Finline taper from a rectangular waveguide to slotline

[1]Ashok Mittal is currently working at Central Research Laboratory, Bharat Electronics Ltd., Ghaziabad, India.